Int. J. Heat Mass Transfer. Vol. 21, pp. 725–734

0017-9310/78/0601-0725 $02.00/0

THE CONTRIBUTION OF LATENT HEAT TRANSPORT IN SUBCOOLED NUCLEATE BOILING

MILTON S. PLESSET
California Institute of Technology, Pasadena, CA 91125, U.S.A.

and

ANDREA PROSPERETTI
Istituto di Fisica, Università Degli Studi, Milano, Italy 20133

(*Received* 13 *August* 1976 *and in revised form* 25 *October* 1977)

Abstract—An analysis is developed to determine the importance of latent heat transport in nucleate boiling heat transfer to a subcooled liquid. With the aid of experimental data in water for individual bubble radius vs time behavior, the total amount of latent heat transported through the bubble during its lifetime is calculated, and this latent heat is significantly less than the measured heat transfer per bubble. It is concluded that microconvection is the important mechanism for the enhanced heat transfer observed in subcooled water. The results presented here apply only to highly subcooled liquids where bubble growth and collapse occurs at the heated surface, and not to boiling heat transfer in saturated or nearly saturated liquids. In the latter situation the very different bubble dynamics makes possible a significant contribution from latent heat transport.

NOMENCLATURE

- D, thermal diffusivity of liquid;
- J, vapor flux;
- k, thermal conductivity of liquid;
- L, latent heat;
- p^e, equilibrium vapor pressure;
- p_i, pressure within the vapor bubble;
- Pr, Prandtl number ν/D;
- q, heat flux from heated solid in nucleate boiling;
- Q, total latent heat transported through a bubble;
- R, bubble radius;
- $\mathscr{R}$, universal gas constant divided by the molecular weight;
- S, bubble boundary.

Greek symbols

- α, coefficient of accommodation for evaporation, or condensation;
- δ, microlayer thickness, thickness of liquid layer between bubble base and heated solid;
- δ_0, initial value of δ;
- ρ, liquid density;
- ν, kinematic viscosity of liquid;
- τ, total bubble lifetime.

INTRODUCTION

THE PROBLEM of concern in the present study is the physical mechanism whereby the heat transfer from a solid to a liquid is increased with the onset of boiling. We shall restrict our considerations to subcooled boiling where the bubbles grow and collapse in a steep temperature gradient in times of the order of a millisecond. This situation is quite different from saturated or nearly saturated boiling in which the bubbles do not collapse on the solid wall but are detached from it by buoyancy forces after a monotonic growth the duration of which can be tens of milliseconds.

It is generally recognized that heat transfer from a solid to a liquid is limited by the presence of a viscous liquid layer adjacent to the surface. The incremental effect of boiling on the heat transfer is thought to arise because of a specific mechanism which decreases the importance of this large thermal resistance. Two such mechanisms have been proposed. According to the first, which may be called "microconvection in the sublayer", the rapid bubble motion disrupts the stagnant liquid layer by forcing the hot liquid away from the wall during the growth phase, and bringing cold liquid in contact with it upon collapse [1, 2]. The second mechanism supposes that latent heat is transported through the bubble from the hotter regions near the bubble base where liquid evaporates to the colder regions near the pole of the bubble where vapor condenses. The increase in heat transfer then takes place because the latent heat is deposited sufficiently far from the solid wall that turbulent transport can be effective [3–7].

That this mechanism in principle can be very significant becomes clear once it is realized that the no-slip condition, which real fluids must satisfy at a rigid boundary, requires that a liquid layer remain between the base of the bubble, as it grows and collapses, and the solid surface (Fig. 1). If the measured time-average temperature distributions in subcooled boiling [1, 2, 9, 10] are taken to apply to the liquid on the bubble cap, and if the viscous microlayer is taken to be at the temperature of the wall, a temperature difference as large as 60°C to 70°C could exist between the hotter and colder portions of the bubble surface.

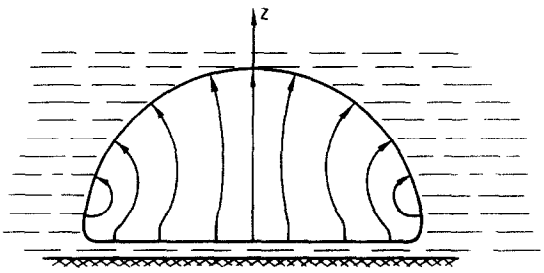

FIG. 1. A schematic representation is shown of the vapor bubble with vapor flow lines.

Many studies have shown that latent heat transport is a significant factor in saturated or nearly saturated boiling [8–31, 37, 39] and also possibly near burnout conditions [32]. For subcooled boiling with bubble growth and collapse, however, there is hardly any experimental evidence regarding latent heat transport [6, 8], and only theoretical studies exist the accuracy of which is subject to serious question [4, 5]. In this paper we propose to make a simple theoretical analysis of the importance of latent heat transport in subcooled nucleate boiling. Our starting point is the observation that the vapor mass flux from a liquid surface is primarily a function of the surface temperature and of the vapor pressure acting on it [33–35]. The internal vapor pressure can be estimated in an unambiguous way from the observed radius vs time data of the bubble growth and collapse, and the temperature at the bubble base can be determined if the simplifying assumption is adopted that the microlayer maintains a uniform thickness which decreases with time by evaporation. Our conclusion is that latent heat transport cannot account for more than 10–15% of the experimental heat transfer associated with each bubble for subcooled boiling in water. This result is essentially a consequence of the drastic reduction in the temperature differences which might otherwise exist over the bubble boundary. These temperature differences are reduced by the relatively slow diffusion of heat from the bubble to the liquid in the short time scale of the bubble life.

Finally, we would like to stress that our negative findings on the importance of microlayer evaporation do not bear on saturated or only slightly subcooled boiling. The basic difference here is that the thickness of the viscous microlayer is not much different from that encountered in subcooled boiling but the time available for heat diffusion prior to bubble detachment is orders of magnitude greater.

FORMULATION OF THE PROBLEM

The development of the viscous microlayer represents in principle a well-defined theoretical problem which, however, has not yet been amenable to a satisfactory analytical treatment in spite of several attempts [22, 36]. Experimental information is also insufficient for our purposes since the only available measurements refer to conditions of saturated or nearly saturated boiling [22, 26, 37]. In view of this situation we make the assumption, which gives a considerable simplification, that the viscous microlayer at the base of the bubble maintains a uniform thickness $\delta(t)$ at all times. This assumption is admittedly rather crude, and we present a discussion of the errors which it may cause below. We also make the assumption that the liquid temperature at the surface of the microlayer exposed to the vapor, $T_b(t)$, is uniform. If $p_i(t)$ is the internal bubble pressure, then it is known [33–35] that the vapor mass flux, J, from the microlayer surface is given by

$$J = \alpha(2\pi\mathscr{R}T_b)^{-1/2}[p^e(T_b) - p_i(t)], \tag{1}$$

where α is the accommodation coefficient for condensation (or evaporation), $\mathscr{R}$ is the universal gas constant divided by the molecular weight of the vapor, and $p^e(T)$ is the equilibrium vapor pressure at temperature T. The accommodation coefficient has been set equal to unity in the computations, which possibly also tends to overestimate the contribution of the latent heat transport.

The above considerations allow us to write the following equation for the microlayer thickness

$$\frac{\mathrm{d}\delta}{\mathrm{d}t} = -\frac{J}{\rho}, \tag{2}$$

where ρ is the liquid density. If Q is the total latent heat extracted from the bubble base, we have also

$$\frac{\mathrm{d}Q}{\mathrm{d}t} = \pi R^2 L J. \tag{3}$$

where L is the latent heat of evaporation.

The surface temperature T_b is determined from the solution of the heat diffusion equation in the microlayer subject to the boundary condition

$$-k\frac{\partial T}{\partial z} = LJ,$$

at the microlayer surface, $z = \delta(t)$. In this equation k is the liquid thermal conductivity and z is the coordinate normal to the solid boundary; heat conduction in the vapor has been neglected. The appropriate boundary condition on the solid surface, $z = 0$, would be the continuity of heat fluxes with the temperature of the solid prescribed at infinity. On the basis of some preliminary computations in which the transient heat conduction in the solid was treated by an integral method, it was concluded, however, that for materials of large thermal conductivity like steel these effects are negligible. Therefore we have taken $T(z = 0, t) = T_w$, a constant, in the computation described in the following. The transient heat-conduction problem in the liquid has been treated by an integral method in the usual way [38] assuming a parabolic temperature profile

$$T(z,t) = T_b(t) + a\frac{\delta - z}{\delta - l} + b\left(\frac{\delta - z}{\delta - l}\right)^2 \tag{4}$$

in the region $l \leqslant z \leqslant \delta$, and $T = T_w$ in $0 \leqslant z \leqslant l$. Here $\delta(t) - l(t)$ is the thickness of the thermal boundary layer in the liquid, and the quantities $a(t)$ and $b(t)$ are

determined from the boundary conditions specified above to which the following have been added:

$$T(z,0)=T_w,\quad \frac{\partial T}{\partial z}=0 \text{ at } z=l(t).$$

Substituting (4) into the heat equation and integrating over z from $l(t)$ to $\delta(t)$, one obtains then the following equations:

$$\frac{dT_b}{dt}=\frac{3J^2[(T_w-T_b)/\rho-DL/k]-\frac{\partial T}{\partial t}(\delta-l)(T_w-T_b)}{2(k/L)(T_w-T_b)+(\delta-l)\left|J+\frac{\partial T}{\partial T_b}(T_w-T_b)\right|}; \tag{5a}$$

$$\frac{dl}{dt}=\frac{1}{3}\left|2(k/L)+(\delta-l)\frac{\partial T}{\partial T_b}\right|\frac{dT_b}{dt}-\frac{J}{\rho}+\frac{1}{J}\frac{\partial T}{\partial t}(\delta-l). \tag{6}$$

These equations are only valid as long as $l(t)>0$. When this condition ceases to be satisfied, use has been made of the following temperature distribution

$$T(z,t)=T_b(t)+c\frac{\delta-z}{\delta}+d\left(\frac{\delta-t}{\delta}\right)^2,$$

which in a similar way leads to

$$\frac{dT_b}{dt}=\frac{[J\delta+(k/L)(T_w-T_b)]J/\rho-\frac{1}{2}\delta^2\frac{\partial J}{\partial t}+6D[(k/L)(T_w-T_b)-J\delta]/\delta}{\delta\left|2k/L+\frac{1}{2}\delta\frac{\partial J}{\partial T_b}\right|}. \tag{5b}$$

It was found that the switch from (5a) to (5b) when $l(t)$ became zero did not result in any appreciable discontinuity in the derivative of the temperature of the bubble base.

A relation for $p_i(t)$ is necessary to close the system of equations presented above. It was shown in [35] that, if $T(x,t)$ is the instantaneous temperature distribution over the bubble surface, the internal bubble pressure is approximately given by

$$p_i(t)=\frac{\int_{S(t)}T^{-1/2}p^e(T)\,dS}{\int_{S(t)}T^{-1/2}\,dS}\simeq\frac{1}{S}\int_{S(t)}p^e(T)\,dS, \tag{7}$$

where the integrals are performed over the entire bubble surface $S(t)$. To use this result it is necessary to determine $T(x,t)$, a task which would require some lengthy computations but which appears to be feasible with suitable approximations. In the present study we have chosen a simpler approach which relies on measured data of the bubble dynamics. If it is assumed that, aside from the viscous microlayer, viscous effects are unimportant in the vapor bubble growth and collapse and that, as shown by experiments for the high heat fluxes [17] of present concern, the bubble is hemispherical, the following well-known relation exists between the internal pressure and the bubble radius $R(t)$, and its time derivatives:

$$R\frac{d^2R}{dt^2}+\frac{3}{2}\left(\frac{dR}{dt}\right)^2=\frac{1}{\rho}\left|p_i(t)-p_\infty-\frac{2\sigma}{R}\right|. \tag{8}$$

Here σ is the surface tension and p_∞ the ambient pressure, which we take to be a constant. This equation enables one to compute $p_i(t)$ once $R(t)$ is known. To this end we shall rely mainly on the data of Gunther and Kreith [1, 2], examples of which are shown in Fig. 2, and also on the data of Gunther [40]. While these experiments date back some years ago, they were conducted under carefully controlled conditions, and provided simultaneously information on bubble radii as function of time, heat flux, wall temperature, and average temperature profile in the neighborhood of the heated solid. This last piece of information will be of interest for comparison with the pressure-averaged temperature distribution over the bubble cap, $T_{av}(t)$, defined by

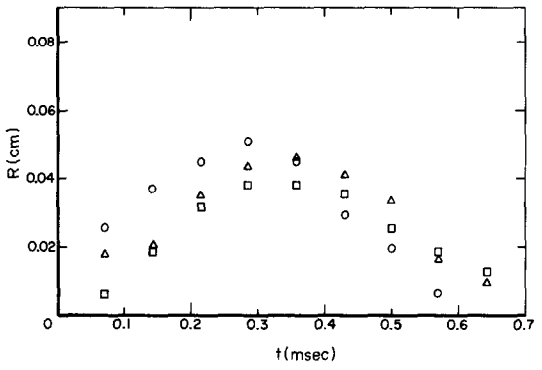

FIG. 2. Some measured values of bubble radii as functions of time from [1]. The (average) solid wall temperature is 132.2°C (270°F), the bulk liquid temperature is 36.7°C (98°F), the heat flux is 3.26 MW/m² (2 Btu/in² s), and the ambient pressure is 1 atm. The liquid temperature data for these same conditions are shown in Fig. 11.

$$p^e(T_{av})=\frac{1}{R(t)-\delta(t)}\int_{\delta(t)}^{R(t)}p^e(T)\,dz. \tag{9a}$$

The RHS of equation (9a) is the average of the equilibrium vapor pressure over the bubble cap; the temperature T_{av} is defined as the temperature for which

the equilibrium vapor pressure is equal to this average pressure. From (7) one readily obtains

$$p^e(T_{av}) = \tfrac{3}{2}p_i - \tfrac{1}{2}p^e(T_b). \tag{9b}$$

It should be noted that T_{av} represents an overestimate of the average cap temperature because of the monotonically increasing behavior of the function $p^e(T)$.

RESULTS

The continuous line in Fig. 3 shows a fit to a typical set of radius vs time data of a bubble observed by Gunther and Kreith [1, 2]. The data are shown by open circles both in Fig. 2 and in Fig. 3. The

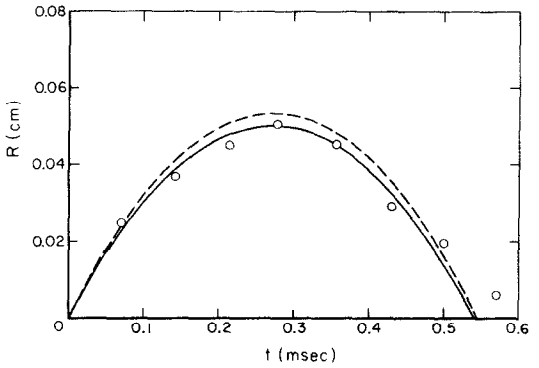

FIG. 3. The circles are observed values for bubble radius, $R(t)$, from Gunther and Kreith [1]. The solid line is the fit to the data used in the analysis here; the dashed line is a second fit used to study the sensitivity of the analysis to the $R(t)$ values used.

experimental conditions for these data were $T_w = 132.2°C$ (270°F), bulk liquid temperature $T_\infty = 36.7°C$ (98°F), heat flux $q = 3.26\,MW/m^2$ (2 Btu/m^2 s). When this fit is used to compute the bubble internal pressure, the quantity $Q(\tau)$ can be computed by integration of the system of equations (2), (3), (5) and (6) shown above. The results of this computation are shown in Fig. 4 as a function of the parameter δ_0. It is seen that the curves for $Q(\tau)$ flatten off at about $\delta_0 = 0.7 \times 10^{-3}$ cm, implying that further increase in the initial thickness does not appreciably affect the amount of latent heat transport. For these thick microlayers the only source of energy is the microlayer superheat itself with the heated wall giving practically no contribution on the time scale of the bubble lifetime which, for the present example, was 0.54 ms. The effect of the wall as a heat source makes itself evident for $\delta_0 \sim 0.5 \times 10^{-3}$ cm, and the total latent heat transported rises with decreasing δ_0. The decline from the peak for smaller δ_0 is a consequence of the onset of dryout of the microlayer prior to bubble collapse.

On the basis of dimensional considerations we may expect for this case a value of δ_0 of the order of $(\frac{1}{2}\nu\tau)^{1/2} \simeq 0.9 \times 10^{-3}$ cm where ν denotes the kinematic viscosity of water. This estimate also agrees with the expression given by Cooper and Lloyd [22]. The corresponding value of $Q(\tau)$ is found to be 6.5×10^3 ergs. From the observed bubble populations

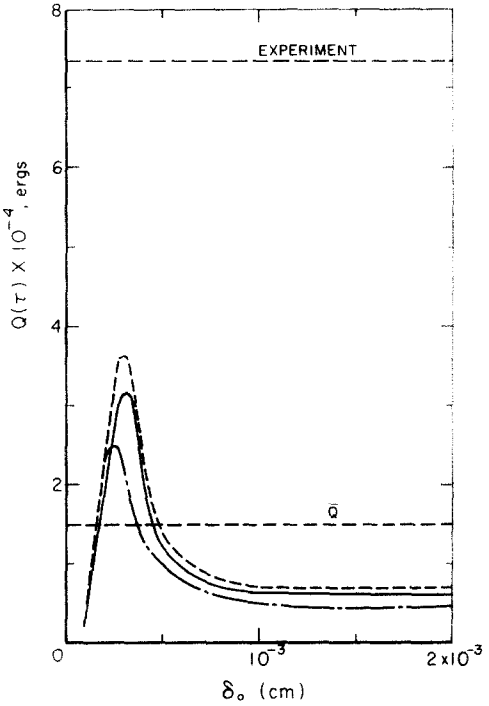

FIG. 4. The calculated total heat, $Q(\tau)$ in ergs, extracted from the microlayer is shown as a function of the mean initial thickness, δ_0, of the microlayer. The solid line is the result of $R(t)$ given by the solid line of Fig. 4, the dashed line is the result for the $R(t)$ given by the dashed line of Fig. 3; the dash–dot line is for a solid wall temperature reduced by 5°C with the $R(t)$ given by the solid line. The horizontal lines are the experimental value of the heat transport per bubble and the value of $\bar{Q}$ calculated from (12).

and frequencies, Gunther and Kreith have estimated the average contribution of each bubble to the total heat transfer to be of the order of 7.4×10^4 ergs which is an order of magnitude greater than the latent heat transport just found. Figure 4 shows that latent heat transport could be more significant only if δ_0 were in a relatively narrow band around 0.3×10^{-3} cm, a value which appears to be unrealistically small.

The details of the results of Fig. 4 depend on the fit of the $R(t)$ data used and on the wall temperature. This dependence is illustrated in the figure by the two broken lines. The upper one was obtained with the $R(t)$ fit shown as a dashed line in Fig. 3; the lower broken line is the result for a wall temperature 5°C lower, i.e. $T_w = 127.2°C$. It is apparent that our conclusions would remain unchanged even with such changes in these input data.

It is of some interest to analyze in a similar way another of the bubbles measured by Gunther and Kreith in water for a heat flux twice the previous one, $q = 6.25\,MW/m^2$ (4 Btu/in^2 s). The wall temperature was 136.3°C (277.5°F) and the bulk liquid temperature $T_\infty = 14.4°C$ (58°F). The radius–time data and the fit used in the calculations are shown in Fig. 5. Figure 6 illustrates the behavior of $Q(\tau)$ for different δ_0. If the considerations in favor of the latent heat transport mechanism outlined in the introduction were valid, one would expect to find larger values of $Q(\tau)$ than in

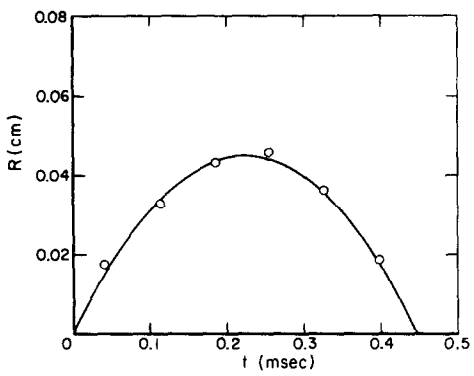

FIG. 5. The circles give observed values of $R(t)$ from Gunther and Kreith [1] for a heat flux twice that of Fig. 3.

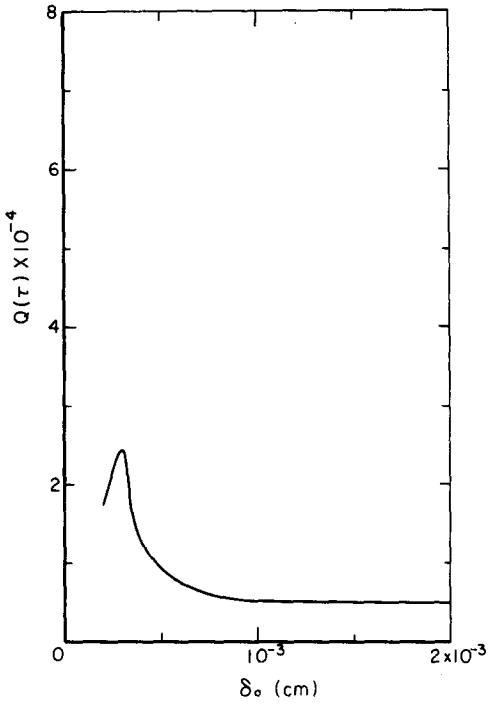

FIG. 6. The calculated total heat, $Q(\tau)$ in ergs, extracted from the microlayer is shown as a function of the mean initial thickness, δ_0, of the microlayer for the $R(t)$ shown in Fig. 5.

the previous case because of the higher wall temperature and also because of the greater liquid subcooling. As a matter of fact the values of $Q(\tau)$ turn out to be lower than before: the somewhat smaller values of the maximum radius and of the bubble lifetime apparently are sufficient to offset the incremental effects of these factors. Although no estimate of the total latent heat transport per bubble is available for this case, our results strongly indicate that the increase in heat flux is produced solely by an increased microconvective effect as a consequence of the greater number of bubbles per unit area and also of the shorter lifetimes and greater frequencies as observed by Gunther [40].

The measurements reported in [40] also include heat transfer, bubble kinematics, and bubble population in forced convection with large subcooling. Unlike the data of Gunther and Kreith, however the reported radius vs time behavior exhibits large differences for different bubbles. Gunther [40] does however give data for the maximum radius and the lifetime of the "average" bubble. Since these data were obtained from a larger sample of bubble histories than those reported in the paper, we have chosen to perform an analysis similar to the preceding one for this "average" bubble. A parabolic fit was found to reproduce in an acceptable way the observed radius vs time data. It appears reasonable, therefore, that a parabolic fit determined (uniquely) in terms of the average maximum radius and average lifetime represents a good approximation to the kinematic behavior of the "average" bubble. In Fig. 7 we present a graph of $Q(\tau)$ vs δ_0

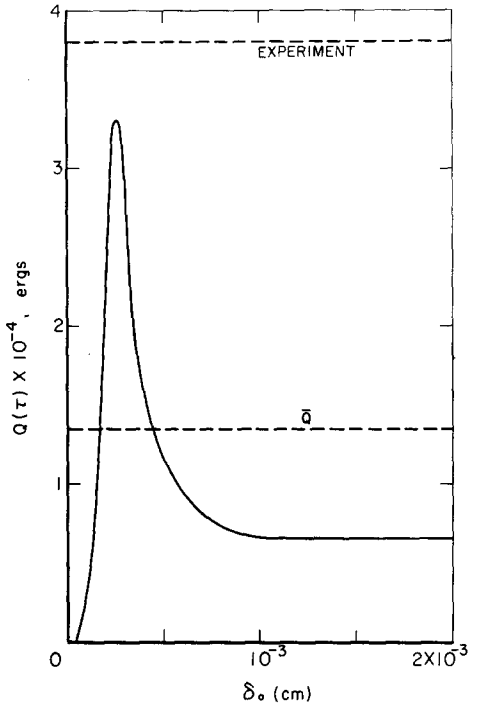

FIG. 7. The calculated total heat, $Q(\tau)$ in ergs, extracted from the microlayer is shown as a function of the mean initial thickness, δ_0, of the microlayer for an $R(t)$ behavior based on the observed values $R_{max} = 3.81 \times 10^{-2}$ cm and $\tau = 0.45 \times 10^{-3}$ s [40]. The heat flux was 4.51 MW/m^2, the liquid velocity 3 m/s, the ambient pressure 0.96 atm, the wall temperature 134°C and the bulk liquid temperature 48.9°C. The horizontal lines are the experimental value of the heat transport per bubble and the value of $\bar{Q}$ calculated from (12).

for the "average" bubble observed at a heat flux of 4.51 MW/m^2 (2.75 Btu/in^2 s), liquid velocity of 3 m/s (10 ft/s), and ambient pressure 0.96 atm. The wall temperature is not reported, but can be estimated from the data of [1] to be 134°C (273.2°F). The average maximum radius was $R_{max} = 3.81 \times 10^{-2}$ cm, the average bubble lifetime 0.45×10^{-3} s, the bulk liquid temperature 48.9°C (120°F), and the estimated heat transfer per bubble 3.8×10^4 ergs. In Fig. 7 we present the results for the latent heat transport analysis in the form of a graph of $Q(\tau)$ vs δ_0 as was done above. For a value of $\delta_0 = (\frac{1}{2}v\tau)^{1/2} = 6.53 \times 10^{-4}$ cm we find $Q(\tau) = 8.5 \times 10^3$ ergs, which is less than 25% of the experimental value. Again one would find a more significant

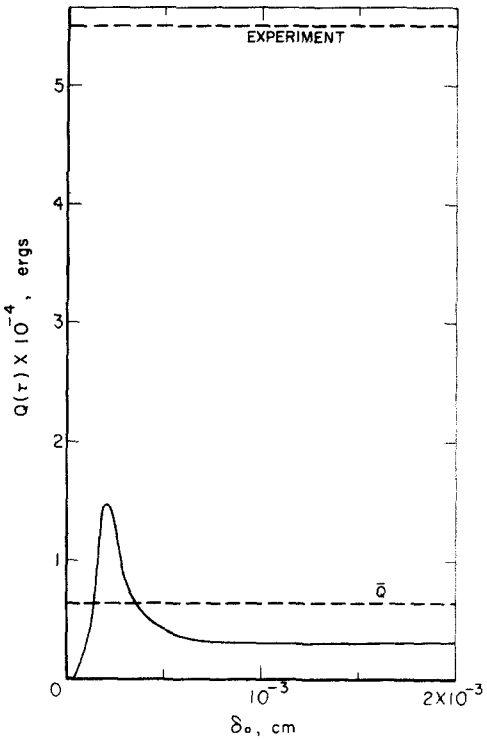

FIG. 8. The calculated total heat, $Q(\tau)$ in ergs, extracted from the microlayer is shown as a function of the mean initial thickness, δ_0, of the microlayer for an $R(t)$ behavior based on the observed values $R_{max} = 3.81 \times 10^{-2}$ cm and $\tau = 0.3 \times 10^{-3}$ s [40]. The heat flux was 4.51 MW/m^2, the liquid velocity 3 m/s, the ambient pressure 0.96 atm, the wall temperature 134°C and the bulk liquid temperature 26.7°C. The horizontal lines are the experimental value of the heat transport per bubble and the value of $\bar{Q}$ calculated from (12).

effect of latent heat transport only for narrowly restricted values of δ_0 around the small value of 2.5×10^{-4} cm. Figure 8 reports the results of a similar analysis performed on the "average" bubble observed by Gunther [40] under the same experimental conditions except for the bulk water temperature which was now much more subcooled, $T_\infty = 26.7$°C (80°F). The observed maximum radius was again $R_{max} = 3.81 \times 10^{-2}$ cm, but the average lifetime was considerably shorter, $\tau = 0.3 \times 10^{-3}$ s. The estimated heat transfer per bubble was 5.5×10^4 ergs, higher than the preceding value because of the smaller number of bubbles per unit area observed in these conditions. It is seen that the peak of the $Q(\tau)$ curve is considerably lowered because of the much shorter bubble lifetime, and that the contribution of latent heat transport is very small indeed.

DISCUSSION

With the hypothesis of axial symmetry the total amount of latent heat transported through the bubble during its lifetime τ is given by

$$Q_{exact} = 2\pi \int_0^{\tau} dt \int_0^{R(t)} rLJ_{exact}(r,t)\,dr. \quad (10)$$

The procedure for evaluating Q indicated in equation (3) corresponds to the neglect of the dependence of J on r in equation (10). It is clear that this approximation, which was justified with the assumption of a microlayer of uniform thickness, represents a rather crude oversimplification of the real process. The thickness of the microlayer on the bubble base increases in the radial direction due to a combination of several effects: first, the increase in the distance from the center of the bubble (which in the present geometry plays the role of the leading edge for a two-dimensional viscous boundary); second, the decrease in bubble growth velocity with time; third, the different exposure times to evaporation of the various portions of the bubble base. Thus, the initial microlayer thickness will span a range of values from 0 to some finite value at the edge of the bubble, and a dry patch will form at the center of the bubble and expand radially with time.

In order to estimate the effect associated with this nonuniformity of the initial microlayer thickness we proceed as follows. A straightforward change in the order of integration of the two-dimensional integral in (10) gives

$$Q_{exact} = 2\pi \int_0^{R_{max}} r\,dr \int_{t_g(r)}^{t_c(r)} LJ_{exact}(r,t)\,dt. \quad (11)$$

where R_{max} is the maximum bubble radius, and $t_g(r)$ and $t_c(r)$ are the instants of time at which the bubble boundary grows and collapses past the distance r from the bubble center respectively. In view of the fact that the microlayer is thin compared with the radius of the bubble, it is reasonable to assume that conduction effects in the direction normal to the wall will dominate over those in the radial direction so that the various infinitesimal rings that make up the bubble base effectively behave independently of one another. In this approximation, given the bubble kinematics, the inner integral in (11) depends only on the initial microlayer thickness at the distance r from the bubble center. Dimensional considerations and the results of Cooper and Lloyd [22] lead us to take $\delta_0 = [vt_g(r)]^{1/2}$ for this initial thickness. We now use the mathematical model described above to compute the inner integral for various values of δ_0 and use the trapezoidal rule to compute the following approximation to Q_{exact}

$$\bar{Q} = 2\pi \int_0^{\delta_{max}} r \frac{dr}{d\delta_0}\,d\delta_0 \int_{t_g}^{t_c} LJ(\delta_0,t)\,dt, \quad (12)$$

where $\delta_{max} = \delta_0(R_{max})$. The results for the different bubbles analyzed by us are indicated by horizontal lines in Figs. 4, 7 and 8. In general it is seen that the value of $\bar{Q}$ represents an average of the values of $Q(\tau)$ which in all cases is considerably below the maximum. Estimating the importance of latent heat transport with $\bar{Q}$ we find a contribution of 21, 36 and 12% respectively for the bubbles of Figs. 4, 7 and 8. Only the second result, obtained with the smallest subcooling, indicates a significant contribution of latent heat transport to the total heat transfer per bubble. From combining these conclusions with those obtained by others in the case of saturated or only slightly subcooled boiling, it appears then that the importance of latent heat transport decreases with increasing sub-

cooling, contrary to the expectations commonly held. A consideration of the results of Figs. 7 and 8 shows that this behavior depends essentially on the shorter bubble lifetimes associated with increasing subcooling, coolant velocity and, in a certain range, heat fluxes (cf. [40]). Near burnout the exposure time to evaporation of the liquid microlayer increases again, thus rendering possible a significant contribution of latent heat transport as was estimated by Bankoff [32].

The method used above to estimate Q_{excess} in terms of Q is certainly not entirely satisfactory. The most serious source of error appears to be the fact that in reality when a fresh portion of microlayer is exposed to evaporation, all the liquid in it will be at a temperature close to T_w. On the contrary, our computational model attributes to this liquid the same temperature distribution that has been established at the center of the microlayer during the preceding bubble lifetime. As a consequence we make an error both in the initial surface temperature and in the superheat content of the fresh portion of microlayer. It is clear, however, from Fig. 10 that the surface temperature drops to the value it has at the other points in a time of the order of 10^{-6} s, which is much shorter than the bubble lifetime, so that the first element of error appears to be of negligible consequences. This is not so for the second one, however, and we need a more careful analysis to estimate its importance. The latent heat necessary to vaporize the microlayer comes from two sources, the microlayer superheat and the wall. In order to assess the relative importance of these two contributions we may consider the ratio $Q_s/Q(\tau)$, where Q_s is the microlayer superheat, as a function of δ_0. A simple estimate of Q_s is given by

$$Q_s = \pi R_{\max}^2 c\rho(T_w - T_B)\delta_0, \qquad (13)$$

where c is the specific heat and T_B is the boiling temperature at the ambient pressure, which is also the average liquid temperature at the microlayer surface (see Fig. 11 below). It should be realized that (13) is an upper bound on the liquid superheat actually available for evaporation. We present in Fig. 9 a plot of the ratio $Q_s/Q(\tau)$ as a function of δ_0 for the bubble of Figs. 3 and 4; a similar behavior is observed in the other cases. Comparison with the graph of Fig. 4, showing $Q(\tau)$ as a function of δ_0, shows that the liquid superheat becomes a significant factor only for values of δ_0 so large that $Q(\tau)$ is but a small fraction of the experimental value. These arguments lead to the conclusion that heat conduction from the wall is the determining effect in microlayer evaporation so that also the second source of error in the computation of Q indicated above does not appear likely to have a considerable influence on our conclusions.

The present results are at variance with those of Snyder and Robin [4, 5]. These authors have attempted to give a more elaborate analysis than was done here, incorporating the heat transfer from the bubble cap to the turbulent stream, and have obtained results on the basis of which nearly 100% of the total heat transfer could be attributed to latent heat transport. The mathematical formulation used by Snyder and Robin is so complex that a certain number of assumptions and approximations have necessarily been introduced which, however, are not too clear from their papers. It is therefore difficult to judge exactly why their results are so different from ours. There are two specific points in their analysis, however, which appear to be subject to serious question. First, the latent heat of vaporization and condensation appears in their equations in the form of heat sources or sinks distributed in the liquid, rather than as suitable boundary conditions. The boundary condition used in [4–6] at the liquid surface is one of zero temperature gradient. This boundary condition, $\partial T/\partial r = 0$, could give very large errors since one may easily estimate $\partial T/\partial r$ and find that it is of the order of 10^4 °C/cm, and a small error in the interface temperature leads to large errors in J. Second, they made the assumption of uniform vapor density in the bubble which would also introduce an error in their equation for the vapor mass flux. The present analysis is made much simpler and more direct by recourse to the measured values for $R(t)$ to compute the internal pressure in the vapor bubbles.

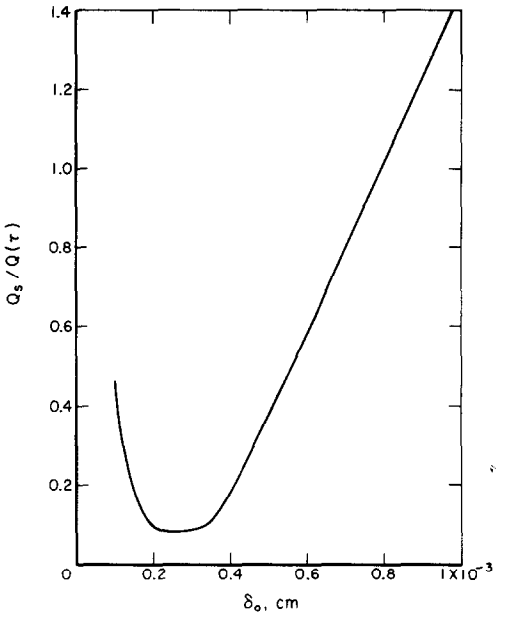

FIG. 9. The ratio of the superheat content (13) of the microlayer to the calculated $Q(\tau)$ is shown as a function of the initial microlayer thickness δ_0 for the bubble of Figs. 3 and 4.

FURTHER COMMENTS ON LATENT HEAT TRANSPORT

The results outlined in the previous section appear quite surprising in view of the very large temperature differences that may *a priori* be thought to be available between the base and the cap of the bubble. In order to clarify the physical processes involved we show in Fig. 10 the time dependence for the bubble of Figs. 3–4 of the temperature, T_b, of the vapor boundary of the microlayer. It may be observed that for all values of δ_0 there is an extremely rapid decrease in T_b from 132.2 to 108°C in less than 5×10^{-6} s, followed by a further

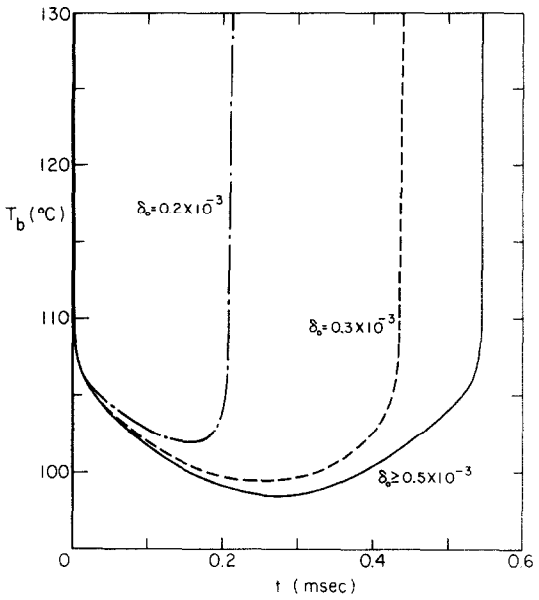

FIG. 10. The liquid temperature of the microlayer, T_b, at the bubble interface is shown as a function of time for the bubble of Fig. 3 for various values of average initial microlayer thickness, δ_0.

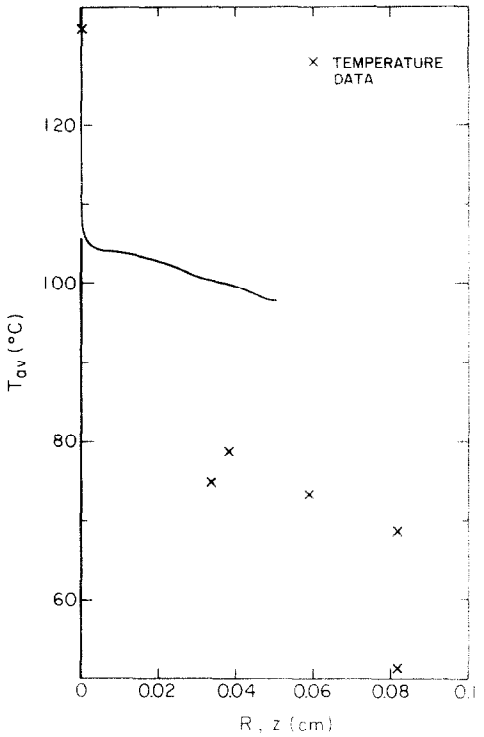

FIG. 11. The pressure-averaged temperature for the bubble cap, for the bubble of Fig. 3, is shown as a function of bubble radius R. The crosses show the temperature data reported by Gunther and Kreith [1, 2] as a function of distance, z, from the solid wall.

decrease which, for $\delta_0 \leqslant 5 \times 10^{-4}$ cm, depends on the value of δ_0. If δ_0 is small enough for the wall to be effective, T_b recovers before the bubble collapse and reaches its initial value T_w very rapidly just before microlayer dryout. For larger values of δ_0, however, the microlayer surface temperature remains close to the boiling point throughout most of the bubble lifetime.

It would be very interesting to have similar results for the temperatures on the bubble cap. Unfortunately only limited information is available here, namely, the pressure-averaged cap temperature defined by equation (9), T_{av}. This quantity is shown in Fig. 11, again for the bubble of Figs. 3–4 and for the case $\delta_0 = 5 \times 10^{-4}$ cm. This figure is actually a cross-plot of the two relations $T_{av}(t)$ and $R(t)$ during the growth portion of the bubble lifetime. In this way each point on the curve gives the average cap temperature at the instant at which the bubble radius is $R = R(t)$. This cross-plot of these two functions of time affords an interesting comparison of the variation of the liquid temperature with distance, z, from the wall as measured by Gunther and Kreith [1, 2], whose data are also shown in Fig. 11. Indeed, it might be thought that T_{av} is obtainable from these measured values, but it is clear from the figure that this is not the case. T_{av} decreases very rapidly at first, and remains nearly constant afterwards. Apparently the fact that the bubble cap during its growth penetrates into colder and colder liquid is of little importance in the temperature distribution that is established over it.

From Figs. 10 and 11 it may be concluded that, rather than providing a "short circuit" for the heat flow as has been suggested [4], the transport of vapor in the bubble has the effect of short-circuiting the temperature distribution over its surface. An important consequence of this behavior is that it tends to reduce considerably the possible role of thermocapillary phenomena, which are sometimes introduced to explain several features of boiling phenomena [41].

As Fig. 10 shows, the statement about temperature equalization just made is valid only if the microlayer is sufficiently thick to moderate the effect of the wall. It is possible to give a rough estimate of the conditions under which this situation will take place by observing that, if τ_g denotes the growth time of the bubble, the microlayer thickness will be of the order of $(\nu\tau_g)^{1/2}$. On the other hand, if the surface of this microlayer remains exposed to the vapor for a time τ_c, the penetration distance for the cooling effect of vaporization into the microlayer will be of the order of $(D\tau_c)^{1/2}$. For a subcooled boiling bubble which grows and collapses, τ_g and τ_c are of the same order, so that the condition for the wall effect to be important is that

$$\left(\frac{\nu}{D}\right)^{1/2} = Pr^{1/2} \ll 1, \tag{14}$$

where Pr is the Prandtl number. The Prandtl number for water in the temperature range of present interest is about unity, so that the condition of equation (14) is not met. We may conclude that we cannot expect a substantial contribution to heat flow by latent heat transport in subcooled boiling of water. The implication is that the enhancement of the heat flux from nucleate boiling in liquids like water comes primarily from the intimate mixing effect of the microconvection

generated by the vapor bubble growth and collapse. One might expect that a liquid with small Prandtl number, such as liquid sodium, would have an important contribution to heat flux from latent heat transport in nucleate boiling. There is, however, an effect which tends to reduce this contribution, namely, a strong reduction in the temperature gradient in the liquid because of the large thermal conductivity of sodium. This behavior reduces the available temperature difference over the bubble.

We may note also that in the case of saturated or nearly saturated boiling in water, for which the bubbles do not collapse but detach from the wall, one has $\tau_g < \tau_e$, so that equation (14) does not apply. This observation explains why such a significant contribution from latent heat transport has been found under these conditions.

Although negligible as a direct mechanism of heat transfer in subcooled boiling, latent heat transport still plays a determining, if more indirect, role. It is easy to show on the basis of equation (8) that bubbles would not be expected to grow beyond the distance from the heated wall at which the liquid temperature equals the boiling temperature at the prevailing ambient pressure. The observed bubble growth beyond this region [9] remains inexplicable until it is recognized that the bubble cap is heated by the condensing vapor flux. As equation (7) shows, the pressure level in the bubble can then remain sufficiently high to produce the relatively large maximum radii observed. This explanation appears more convincing than one often put forward according to which the growing bubble carries along a portion of the superheated liquid layer adjacent to the wall. The obvious difficulty with this explanation is that the behavior in question is observed also in flow boiling of highly subcooled liquids in which an appreciable relative velocity exists between the bubble and the liquid stream [9, 40]. It is clear that the larger size attained by the bubbles by this mechanism has an incremental effect on the microconvective heat transfer inasmuch as it decreases the average temperature of the liquid brought in contact with the wall upon collapse.

Acknowledgements—The authors express their appreciation to the Referee who with his criticisms has helped them to formulate more clearly the content of this paper and has lead them to include a more detailed discussion of the approximations involved.

The study was supported by the National Science Foundation under Grant No. ENG 75-22676.

REFERENCES

1. F. C. Gunther and F. Kreith, Photographic study of bubble formation in heat transfer to subcooled water, Progress Report No. 4-120, Jet Propulsion Laboratory, Pasadena (1950).
2. K. E. Forster and R. Greif, Heat transfer to a boiling liquid-mechanism and correlations, *J. Heat Transfer* **81C**, 43–53 (1959).
3. S. G. Bankoff, W. J. Colahan Jr. and D. R. Bartz, Summary of conference on bubble dynamics and boiling heat transfer, Memo 20-137, Jet Propulsion Laboratory, Pasadena (1956).
4. N. W. Snyder and T. T. Robin, Mass-transfer model in subcooled nucleate boiling, *J. Heat Transfer* **91C**, 404–412 (1969).
5. T. T. Robin and N. W. Snyder, Bubble dynamics in subcooled nucleate boiling based on the mass transfer mechanism, *Int. J. Heat Mass Transfer* **13**, 305–318 (1970).
6. T. T. Robin and N. W. Snyder, Theoretical analysis of bubble dynamics for an artificially produced vapor bubble in a turbulent stream, *Int. J. Heat Mass Transfer* **13**, 523–536 (1970).
7. S. G. Bankoff and R. D. Midesell, Bubble growth rates in highly subcooled nucleate boiling, *Chem. Engng Progr. Symp. Ser.* **29**, 95–102 (1959).
8. S. G. Bankoff and J. P. Mason, Heat transfer from the surface of a steam bubble in a turbulent subcooled liquid stream, *A.I.Ch.E. Jl* **8**, 30–33 (1962).
9. L. M. Jiji and J. A. Clark, Bubble boundary layer and temperature profiles for forced convection boiling in channel flow, *J. Heat Transfer* **86C**, 50–58 (1964).
10. J. R. Wiebe and R. L. Judd, Superheat layer thickness measurements in saturated and subcooled nucleate boiling, *J. Heat Transfer* **93C**, 455–461 (1971).
11. T. F. Rogers and R. B. Mesler, An experimental study of surface cooling by bubbles during nucleate boiling of water, *A.I.Ch.E. Jl* **10**, 656–660 (1964).
12. R. R. Sharp, The nature of liquid film evaporation during nucleate boiling, NASA Technical Note TN D-1997 (1964).
13. R. C. Hendricks and R. R. Sharp, Initiation of cooling due to bubble growth on heating surfaces, NASA Technical Note TN D-2290 (1964).
14. C. Bonnet, E. Macke and R. Morin, Visualisation de l'ebullition nucleé de l'eau a pression atmospherique et mesure simultaneé des variations de temperature des surfaces, European Atomic Energy Community – Euratom, Report EUR 1622 f (1964).
15. N. B. Hospeti and R. B. Mesler, Deposits formed beneath bubbles during nucleate boiling of radioactive calcium sulfate solutions, *A.I.Ch.E. Jl* **11**, 662–665 (1965).
16. N. B. Hospeti and R. B. Mesler, Vaporization at the base of bubbles of different shape during nucleate boiling of water, *A.I.Ch.E. Jl* **15**, 214–219 (1969).
17. M. A. Johnson, J. de la Peña and R. B. Mesler, Bubble shapes in nucleate boiling, *A.I.Ch.E. Jl* **12**, 344–348 (1966).
18. Y. Katto and S. Yokoya, Experimental study of nucleate pool boiling in case of making interference plate approach to the heating surface, in *Proceedings of the 3rd International Heat Transfer Conference*, Vol. 3, pp. 219–227. A.I.Ch.E., New York (1966).
19. K. I. Torikai, Heat transfer in contact area of a boiling bubble on a heating surface, *Bull. Japan Soc. Mech. Engrs* **10**, 338–348 (1967).
20. S. Kotake, On the liquid film of nucleate boiling, *Int. J. Heat Mass Transfer* **13**, 1595–1609 (1970).
21. M. G. Cooper and A. J. P. Lloyd, Transient local heat flux in nucleate boiling, in *Proceedings of the 3rd International Heat Transfer Conference*, Vol. 3, pp. 193–203. A.I.Ch.E., New York (1966).
22. M. G. Cooper and A. J. P. Lloyd, The microlayer in nucleate pool boiling, *Int. J. Mass Transfer* **12**, 895–913 (1969).
23. M. G. Cooper, The microlayer and bubble growth in nucleate pool boiling, *Int. J. Heat Mass Transfer* **12**, 915–933 (1969).
24. M. G. Cooper and R. M. Vijuk, Bubble growth in nucleate pool boiling, in *Proceedings of the 4th International Heat Transfer Conference*, Vol. 5, paper B-2.1. Elsevier, Amsterdam (1970).
25. V. Sernas and F. C. Hooper, The initial vapor bubble growth on a heated wall during nucleate boiling, *Int. J. Heat Mass Transfer* **12**, 1627–1639 (1969).
26. H. H. Jawurek, Simultaneous determination of mic-

rolayer geometry and bubble growth in nucleate boiling, *Int. J. Heat Mass Transfer* **12**, 843–848 (1969).
27. S. J. D. van Stralen and W. M. Sluyter, Local temperature fluctuations in saturated pool boiling of pure liquids and binary mixtures, *Int. J. Heat Mass Transfer* **12**, 187–198 (1969).
28. S. J. D. van Stralen, M. S. Sohal, R. Cole and W. M. Sluyter, Bubble growth rates in pure and binary systems: combined effects of relaxation and evaporation microlayers, *Int. J. Heat Mass Transfer* **18**, 453–467 (1975).
29. H. J. Van Ouwerkerk, The rapid growth of a vapor bubble at a liquid–solid interface, *Int. J. Heat Mass Transfer* **14**, 1415–1431 (1971).
30. V. I. Subbotin, D. N. Sorokin, A. A. Tzyganok and A. A. Gribov, Investigation of vapor bubbles effects on temperature of heat transferring surface at nucleate boiling, in *Proceedings of the 5th International Heat Transfer Conference*, Vol. 4, pp. 55–59. Japan Society of Mechanical Engineers and Society of Chemical Engineers, Tokyo (1974).
31. J. L. Swanson and H. F. Bowman, Transient surface temperature behavior in nucleate pool-boiling nitrogen, in *Proceedings of the 5th International Heat Transfer Conference*, Vol. 4, pp. 60–64. Japan Society of Mechanical Engineers and Society of Chemical Engineers, Tokyo (1974).
32. S. G. Bankoff, A note on latent heat transport in nucleate boiling, *A.I.Ch.E. Jl* **8**, 63–65 (1961).
33. E. H. Kennard, *Kinetic Theory of Gases*. McGraw-Hill, New York (1938).
34. M. S. Plesset, Note on the flow of vapor between liquid surfaces, *J. Chem. Phys.* **20**, 790–793 (1952).
35. M. S. Plesset and A. Prosperetti, Flow of vapor in a liquid enclosure, *J. Fluid Mech.* **78**, 433–444 (1977).
36. R. R. Olander and R. G. Watts, An analytical expression of microlayer thickness in nucleate boiling, *J. Heat Transfer* **91C**, 178–180 (1969).
37. C. M. Voutsinos and R. L. Judd, Laser interferometric investigation of the microlayer evaporation phenomenon, *J. Heat Transfer* **97C**, 88–92 (1975).
38. P. Razelos, Methods of obtaining approximate solutions, in *Handbook of Heat Transfer*, edited by W. M. Rohsenow and J. H. Hartnett, pp. 4–64. McGraw-Hill, New York (1973).
39. R. L. Judd and K. S. Hwang, A comprehensive model for nucleate pool boiling heat transfer including microlayer evaporation, *J. Heat Transfer* **98C**, 623–629 (1976).
40. F. C. Gunther, Photographic study of surface-boiling heat transfer to water with forced convection, *J. Appl. Mech.* **18**, 115–123 (1951).
41. J. G. Collier, *Convective Boiling and Condensation*, p. 165. McGraw-Hill, New York (1972).

LA CONTRIBUTION DU TRANSPORT DE CHALEUR LATENTE EN EBULLITION NUCLEEE SOUS-REFROIDIE

Résumé—On développe une analyse pour déterminer l'importance du transport de chaleur latente dans le transfert thermique par ébullition nucléée vers un liquide sous-refroidi. A l'aide de resultats expérimentaux avec l'eau concernant le rayon d'une bulle unique variable en fonction du temps, on calcule la quantité totale de chaleur latente transportée par la bulle durant sa durée de vie et elle est bien moindre que le transfert thermique dû à la bulle. On conclut que la microconvection est le mécanisme important du fort transfert thermique observé dans l'eau sous-refroidie. Les résultats présentés ici concernent seulement les liquides fortement sous-refroidis dans lesquels la croissance et le collapsus de la bulle se produisent à la paroi chauffée et non pas dans ou près du liquide saturé. Dans cette dernière situation la dynamique très différente de la bulle rend possible une contribution significative du transport de chaleur latente.

DER BEITRAG DES LATENTWÄRME-TRANSPORTS BEIM UNTERKÜHLTEN BLASENSIEDEN

Zusammenfassung—Es ist eine Berechnungsmethode entwickelt worden, um den Einfluß des Latentwärme-Transports bei der Wärmeübertragung beim Blasensieden in einer unterkühlten Flüssigkeit zu bestimmen. Mit Hilfe von experimentallen Daten von Wasser über das zeitliche Verhaltens des Einzelblasenradiusses ist der Gesamtbeitrag des Latentwärme-Transports durch die Blase während ihrer Lebenszeit berechnet worden. Diese Latentwärme ist wesentlich kleiner als die gemessene Wärmeübertragung pro Blase. Daraus läßt sich folgern, daß Mikrokonvektion der wichtigere Mechanismus für die verbesserte Wärmeübertragung in unterkühltem Wasser ist. Die hier vorgelegten Ergebnisse gelten für stark unterkühlte Flüssigkeiten, wobei Blassenwachstum und Blasenzusammenbruch an der beheizten Oberfläche geschehen und nicht für die Wärmeübertragung beim Sieden von gesättigten oder fast gesättigten Flüssigkeiten. Im letzteren Fall ist durch die mannigfaltige Blasendynamik ein wesentlicher Beitrag des Latentwärme-Transports denkbar.

РОЛЬ СКРЫТОЙ ТЕПЛОТЫ ПАРООБРАЗОВАНИЯ ПРИ ПУЗЫРЬКОВОМ КИПЕНИИ С НЕДОГРЕВОМ

Аннотация — Анализируется роль скрытой теплоты парообразования при пузырьковом кипении недогретой жидкости. Для воды, используя экспериментальные зависимости роста радиуса отдельных пузырьков от времени, рассчитывается количество скрытой теплоты парообразования, перенесенной через пузырь за время его существования. Эта скрытая теплота значительно меньше измеренного потока тепла через пузырь. Выяснено, что микроконвекция является важным механизмом интенсификации теплообмена в недогретой жидкости. Результаты данной работы применимы только к сильно недогретым жидкостям, где рост пузырька и его отрыв происходят на нагретой поверхности, а не к теплообмену при кипении в условиях насыщения или близких к насыщению. В последнем случае имеет место совершенно иная динамика пузырька, при которой возможен существенный вклад скрытой теплоты парообразования.